# Magnetic hausmannite from hydrothermally altered manganese ore in the Palaeoproterozoic Kalahari manganese deposit, Transvaal Supergroup, South Africa

J. GUTZMER, N. J. BEUKES

Department of Geology, Rand Afrikaans University, P.O.Box 524, Auckland Park 2006, South Africa

A. S. E. KLEYENSTUBER AND A. M. BURGER

MINTEK, Private Bag X3015, Randburg 2125, South Africa

## Abstract

Hausmannite ($Mn_3O_4$), a manganese oxide with a tetragonally distorted spinel structure, is considered to be ferrimagnetic with a very low Curie temperature of 42.5 K. However, strongly magnetic hausmannite has been discovered in some of the hydrothermally altered high-grade manganese ores of the giant Kalahari manganese deposit in South Africa. EDS-electron microprobe analyses indicate magnetic hausmannite to contain on average between 3 and 11.3 wt.% $Fe_2O_3$. In contrast non-magnetic hausmannite contains on average about 1-3 wt.% $Fe_2O_3$. X-ray powder diffraction analyses reveal small changes in cell dimensions of the magnetic hausmannite related to the high iron content. Mössbauer spectroscopy suggests that all iron is in the trivalent state. Optical microscopy and scanning electron microscopy (electron back-scatter imaging) proved the magnetic hausmannite to be homogeneous in composition, containing only a few minute inclusions of hematite. Magnetic blocking temperatures of the iron-rich hausmannite, approximating the Curie temperature, are of the order of 750 K. It is suggested that the ferrimagnetic state of hausmannite is stabilized and enhanced by replacement of $Mn^{3+}$ by $Fe^{3+}$.

KEYWORDS: hausmannite, Kalahari manganese field, Wessels mine, ferrimagnetism, iron content.

## Introduction

HAUSMANNITE, the manganese oxide ($Mn^{2+}Mn_2^{3+}O_4$) has a tetragonally distorted spinel-type structure. According to Mason (1943) and Frenzel (1980) naturally occurring hausmannite contains up to 6.9 wt.% $Fe_2O_3$. Hausmannite is paramagnetic at room temperature (Frenzel, 1980) and ferrimagnetic below a Curie temperature of between 40 and 45 K (Boucher *et al.*, 1970; Olés, 1976). The magnetic characteristics have been described by Frenzel (1980) to vary only slightly due to increasing content of iron. However, during a study of high-grade manganese ores in the Kalahari manganese field highly magnetic, iron-rich hausmannite was discovered. The magnetic hausmannite is, similar to magnetite and hausmannite, strongly attracted by a hand magnet. This paper documents the geological setting and composition of this unusual hausmannite. Information is also provided on the magnetic properties of the hausmannite.

## Geological setting

The Palaeoproterozoic sedimentary Kalahari manganese field is situated in the Northern Cape Province of South Africa in the Kalahari desert (Fig. 1). The manganese ore beds are interbedded with iron-formation of the Hotazel Formation and preserved in five erosional relict basins. The largest of these erosional relicts covers an area of about 35 km by 15

*Mineralogical Magazine, December 1995, Vol. 59, pp. 703–716*

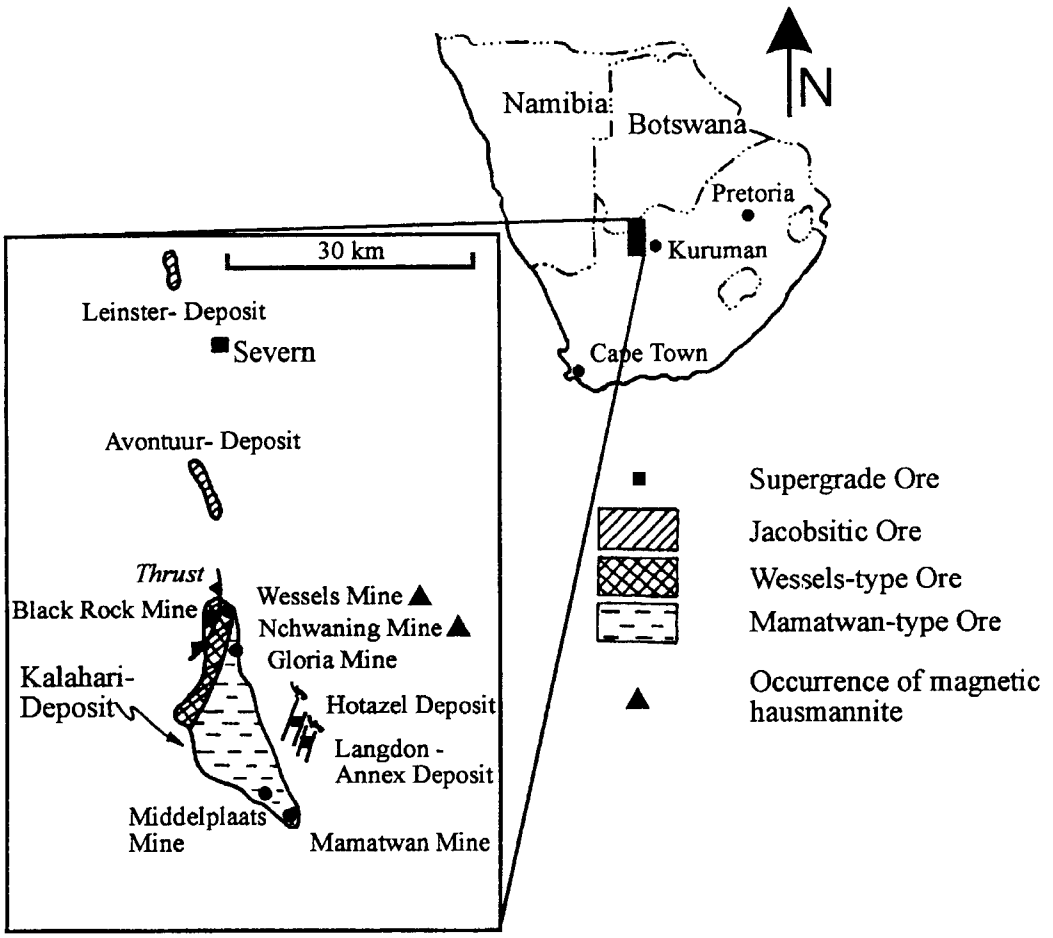


FIG. 1 . Locality map showing the occurrence of magnetic hausmannite relative to the distribution of ore-types, and structural erosionally preserved deposits of the Kalahari manganese field, South Africa (modified after Nel *et al.*, 1986).

km (Fig. 1) and contains the Kalahari manganese deposit with known reserves of about 13500 Mt of manganese ores at grade varying between 20 and 60 wt.% Mn.

Three manganese ore beds are present, each forming the centre of symmetrical iron-formation — hematite-lutite — braunite-lutite sedimentary cycles (Beukes, 1983; Nel *et al.*, 1986). Virtually all manganese ore reserves and production come from the lower manganese bed, which reaches a maximum known thickness of about 45 m in the southwestern part of the manganese field at Mamatwan mine (Fig. 1). Further to the north, at Wessels and Nchwaning mines (Fig. 1), this bed is on average between 4 and 8 m thick.

Two major types of ore are present, namely diagenetic to very low-grade metamorphic sedimentary Mamatwan-type ore and hydrothermally altered Wessels-type ore (Kleyenstüber, 1984). Mamatwan-type ore is of relatively low-grade containing 30–39 wt.% Mn. The ore is microcrystalline, laminated and composed of finely intergrown braunite, hematite, kutnohorite and manganocalcite with abundant small concretionary ovoids of maganese-bearing calcite. Hausmannite is common as a diagenetic oxidation product replacing carbonate ovoids and laminae. This diagenetic/low temperature hausmannite contains up to 4.5 wt.% $Fe_2O_3$ (Nel *et al.*, 1986).

The high-grade Wessels-type ore, containing 46–60 wt.% Mn, was derived from hydrothermal

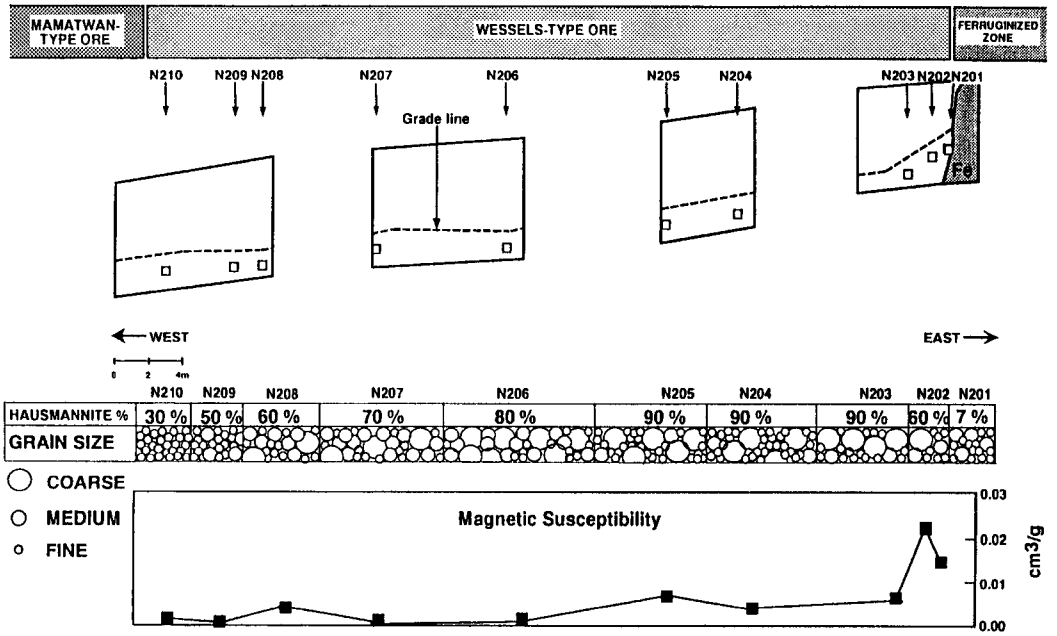


FIG. 2. Sampled traverse at Wessels mine, from unaltered Mamatwan-type ore through Wessels-type ore into a zone of ferruginization surrounding a fault. The hausmannite content, as estimated by optical microscopy, varies from 50% to more than 90% in the samples of Wessels-type ore. Fine-grained magnetic hausmannite and coarse-grained non-magnetic hausmannite are intimately intergrown in variable proportions. A thin hematitic layer, the grade line, was used as reference for height of sampling position. Magnetic susceptibility data for whole-rock samples indicate a large increase towards the zone of ferruginization.

alteration of Mamatwan-type ore in association with a system of normal N–S-trending faults present in the Wessels-Nchwaning area (Gutzmer, 1993; Gutzmer and Beukes, 1993). Only about three percent of the estimated ore reserves are of the Wessels-type and it is concentrated in the intensively faulted northwestern part of the Kalahari deposit (Fig. 1). The normal faults apparently acted as conduits for the hydrothermal fluids leading to hematitization of manganese ores along fault planes and the development of Wessels-type ore adjacent to them (Gutzmer and Beukes, 1993). The high-grade Wessels-type ore is coarse-grained and vuggy composed mainly of hausmannite, bixbyite, braunite II and braunite with minor manganite, marokite and hematite. Gangue minerals include gaudefroyite, andradite, calcite and clinochlore (Kleyenstüber, 1984).

The magnetic hausmannite is associated with a specific part of the Wessels-type ore assemblage. During systematic studies of the metasomatic alteration process from sedimentary Mamatwan-type precursor ore to hydrothermally altered Wessels-type ore, whole rock magnetic susceptibility data were gathered along sample profiles. Unusually high susceptibilities were gained from some hausmannite-rich samples immediately adjacent to ferruginized fault zones (Fig. 2). Tests indicated that in these ores, with high magnetic susceptiblity, a phase of hausmannite could be separated by using a simple hand magnet. In fact one of the authors (A.S.E.K.) found similar strong magnetic hausmannite in a sample from Nchwaning II mine (Fig. 1) in 1986 but at that time the specific geological setting of the material was not realized.

## Petrography and sample preparation

Detailed petrographic studies indicated that very coarse crystalline vuggy hausmannite ores, with hausmannite grain sizes of the order of 0.5–3 mm, do not contain magnetic hausmannite. The magnetic hausmannite is rather developed in massive fine-grained hausmannite-rich ore. This ore-type contains two generations of hausmannite, namely a fine crystalline generation with grain sizes of 100–500 μm, overgrown by younger, very coarse crystalline hausmannite. The fine crystalline hausmannite is

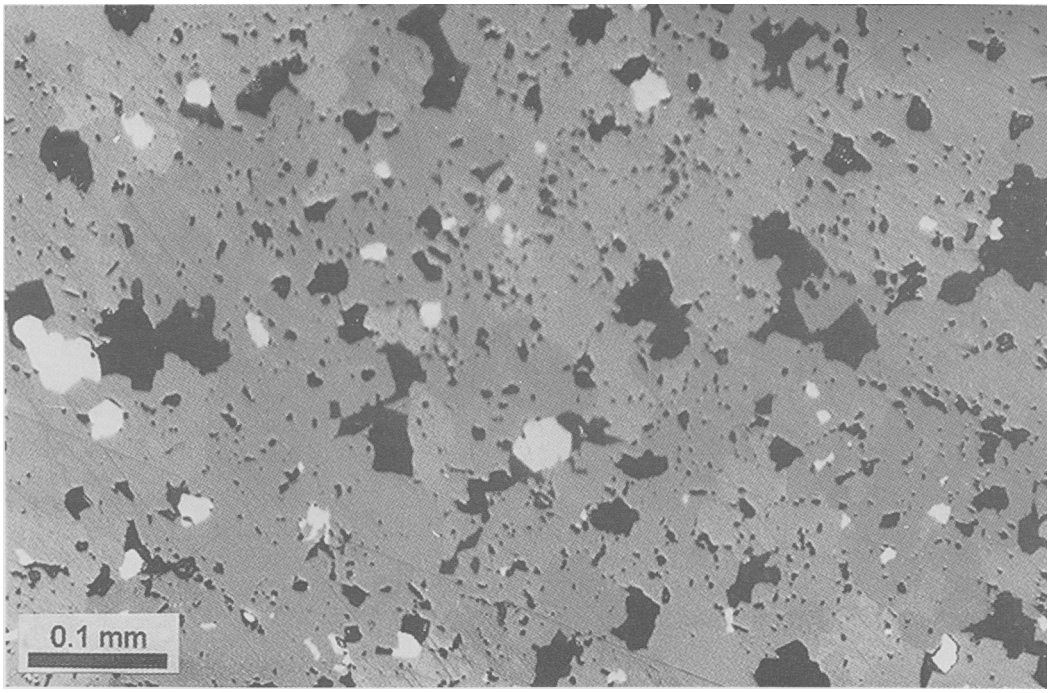


FIG. 3. Reflected light photomicrograph (200 ×, oil immersion) showing typically fine crystalline, anhedral magnetic hausmannite grains (various shades of grey) intergrown with subhedral to euhedral hematite platelets (white).

highly magnetic and attracted by a hand magnet. The coarse crystalline phase does not display this feature.

Minor amounts of bixbyite and braunite II are present in the massive fine-grained magnetic hausmannite-rich ores. Gangue minerals in both magnetic and non-magnetic hausmannite ores include minor hematite, barite, calcite, clinochlore and gaudefroyite.

The intimate intergrowth of the two hausmannite phases in massive ores prohibits complete separation. Samples for chemical, crystallographic and magnetic studies were prepared by stepwise concentration of sieved grain fractions using an isodynamic Frantz magnetic separator. The least magnetic hausmannite fraction was labelled 'non-magnetic', whereas the 'magnetic' fraction was further concentrated by hand-picking magnetic hausmannite grains with a pair of magnetized steel tweezers. However, absolutely pure separates could not be obtained, results of different separates should therefore be regarded as mean values. In addition the properties of some 'non-magnetic' hausmannite, filling vugs in the high-grade ore, have been studied for comparison with the magnetic hausmannite concentrates.

Backscattered electron imaging on mounted grain separates indicated the hausmannite phase to be very pure and of homogenous chemical composition. The only impurities detected were tiny subspherical hematite inclusions of up to 10 μm in diameter (Fig. 3). Careful consideration was given to the possibility that the hausmannites may include minute grains of jacobsite but no such material could be detected. For the same reason X-ray powder diffraction analyses were undertaken. Fine powder for X-ray diffractometry was prepared by milling grain concentrates for 2 minutes in a swingmill and then for 10 minutes in a McCrone micronizing mill using Propan-2-ol as milling medium. X-ray powder mounts were formed by side loading to determine peak intensities and by back loading and pressing to obtain accurate peak positions. For each technique three pellets were prepared and measured independently. Results were averaged.

## Mineral chemistry

Grains of magnetic and non-magnetic separates were analysed with EDS electron microprobe to determine systematic chemical variations. Analyses of Si, Ti, Al, Fe, Mn, Mg, Ca, Na and K indicated that only concentrations of Mn, Fe and Mg are above the detection limit. The mean results from five samples

TABLE 1. Mean composition (electron microprobe) and calculated unit cell constants of pure, iron-free hausmannite and hausmannite containing low, intermediate and high contents of iron

| Sample Separate | Syn. $Mn_3O_4$[a] | Syn. $Mn_3O_4$[b] (this study) | LVB404 low Fe | N204 intermediate Fe | | N205 high Fe | |
|---|---|---|---|---|---|---|---|
| | | | | Magnetic | Non-magnetic | Magnetic | Non-magnetic |
| $Fe_2O_3$ | | | 1.20 | 4.30 | 2.23 | 11.3 | 1.12 |
| $Mn_2O_3$ | 69.0 | 69.0 | 65.2 | 62.7 | 64.5 | 57.1 | 65.8 |
| MnO | 31.0 | 31.0 | 33.1 | 32.7 | 32.6 | 31.8 | 32.6 |
| MgO | | | 0.36 | 0.21 | LLD | LLD | LLD |
| Total | 100.0 | 100.0 | 99.9 | 99.9 | 99.4 | 99.2 | 99.5 |
| Number of analyses | | 1[c)] | 5 | 15 | 9 | 5 | 5 |
| $R$ = (Mn/Mn+Fe) 1 | | 1 | 0.99 | 0.96 | | 0.89 | |
| Unit cell constants | $a_0$= 5.7621 | $a_0$ = 5.764(8) | $a_0$= 5.764(7) | $a_0$ = 5.771(3) | | $a_0$ = 5.772(6) | |
| | $c_0$= 9.4696 | $c_0$ = 9.470(3) | $c_0$ = 9.45(8) | $c_0$ = 9.41(7) | | $c_0$ = 9.41(6) | |
| | $c_0/a_0$ = 1.643 | $c_0/a_0$=1.643 | $c_0/a_0$ = 1.641 | $c_0/a_0$= 1.632 | | $c_0/a_0$= 1.631 | |

a) Values of synthetic $Mn_3O_4$ from National Bureau of Standards (1972).
b) Synthetic hausmannite prepared by heating of $MnCO_3$.
c) Synthetic hausmannite has been wet chemically analysed for Mn and Fe.

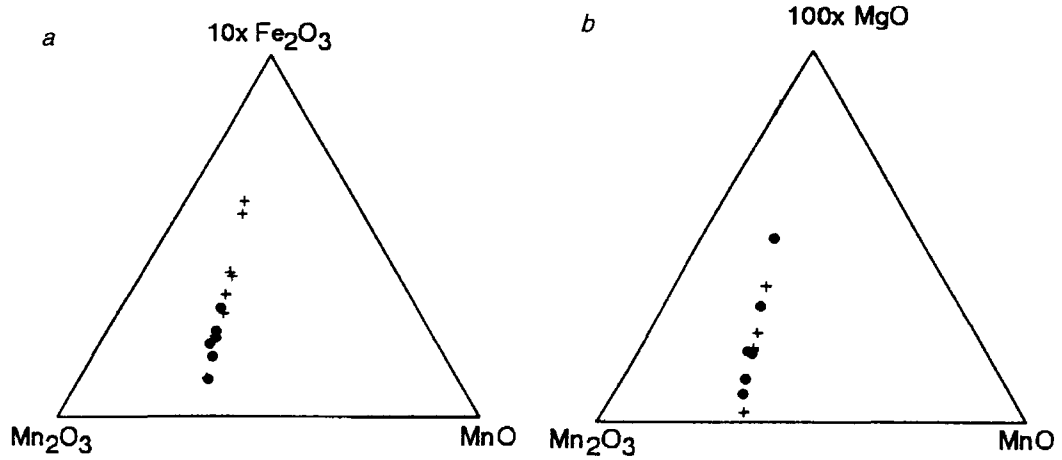


FIG. 4. Mean of EDS-electron-microprobe analyses of magnetic (crosses) and non-magnetic (circles) hausmannite separates from sample profile N200 plotted in triangular diagrams (*a*) $Mn_2O_3$–MnO–10 × $Fe_2O_3$ and (*b*) $Mn_2O_3$–MnO–100 × MgO. Magnetic separates are clearly discriminated from non-magnetic separates by their higher iron content, whereas contents of magnesia are irregularily distributed.

TABLE 2. List of peak positions and relative intensities for magnetic (magnetic separates of N204, N205) and non-magnetic natural (LVB404) and synthetic (MINTEK sample) hausmannite samples. Listed peak positions are corrected and were used to calculate the unit cell constants displayed in Table 1. Position data were aquired using pressed, back-loaded powder mounts, intensity data were obtained from side-loaded powder mounts. Each listed data set represents mean values of measurements on three independently prepared mounts of each sample

| (*hkl*) | Synthetic $Mn_3O_4$ | | LVB404 | | N204 | | N205 | |
|---|---|---|---|---|---|---|---|---|
| | *d* (C) | *I* (rel.) | *d* (C) | *I* (rel.) | *d* (C) | *I* (rel.) | *d* (C) | *I* (rel.) |
| 1 0 1 | 4.918 | 35 | 4.907 | 40 | 4.909 | 54 | 4.913 | 65 |
| 1 1 2 | 3.089 | 48 | 3.084 | 84 | 3.079 | 70 | 3.081 | 65 |
| 2 0 0 | 2.882 | 24 | 2.880 | 32 | 2.882 | 22 | 2.884 | 16 |
| 1 0 3 | 2.768 | 63 | 2.764 | 93 | 2.756 | 100 | 2.756 | 73 |
| 2 1 1 | 2.488 | 100 | 2.487 | 100 | 2.487 | 98 | 2.489 | 100 |
| 2 0 2 | 2.462 | 20 | 2.460 | 7 | 2.458 | 9 | 2.460 | 14 |
| 0 0 4 | 2.367 | 21 | 2.362 | 84 | 2.354 | 62 | 2.353 | 67 |
| 2 2 0 | 2.0385 | 25 | 2.0377 | 40 | 2.0404 | 26 | 2.0398 | 27 |
| 2 0 4 | 1.8296 | 4 | 1.8269 | 6 | 1.8237 | 5 | 1.8232 | 5 |
| 1 0 5 | 1.7993 | 15 | 1.7974 | 22 | 1.7902 | 18 | 1.7905 | 14 |
| 3 1 2 | 1.7010 | 8 | 1.7008 | 7 | 1.7009 | 8 | 1.7025 | 7 |
| 3 0 3 | 1.6417 | 7 | 1.6353 | 5 | 1.6340 | 7 | 1.6376 | 8 |
| 3 2 1 | 1.5766 | 22 | 1.5762 | 26 | 1.5777 | 20 | 1.5783 | 18 |
| 2 2 4 | 1.5449 | 34 | 1.5438 | 59 | 1.5418 | 52 | 1.5433 | 44 |
| 4 0 0 | 1.4411 | 18 | 1.4412 | 32 | 1.4426 | 11 | 1.4428 | 11 |
| 3 0 5 | 1.3489 | 3 | 1.3481 | 3.6 | 1.3579 | 23 | 1.3453 | 3 |
| 4 1 3 | 1.2784 | 6 | 1.2781 | 6 | 1.2787 | 5 | 1.2790 | 5 |
| 4 2 2 | 1.2438 | 4 | 1.2461 | 2 | 1.2452 | 1 | 1.2461 | 1 |
| 4 0 4 | 1.2310 | 4 | 1.2306 | 3 | 1.2304 | 5 | 1.2307 | 5 |
| 0 0 8 | 1.1836 | 2 | 1.1864 | 6 | 1.1920 | 4 | 1.1908 | 4 |
| 4 1 5 | 1.1248 | 4 | 1.1244 | 4 | 1.1242 | 4 | 1.1236 | 4 |
| 4 3 3 | 1.0826 | 4 | 1.0827 | 5 | 1.0834 | 3 | 1.0836 | 4 |

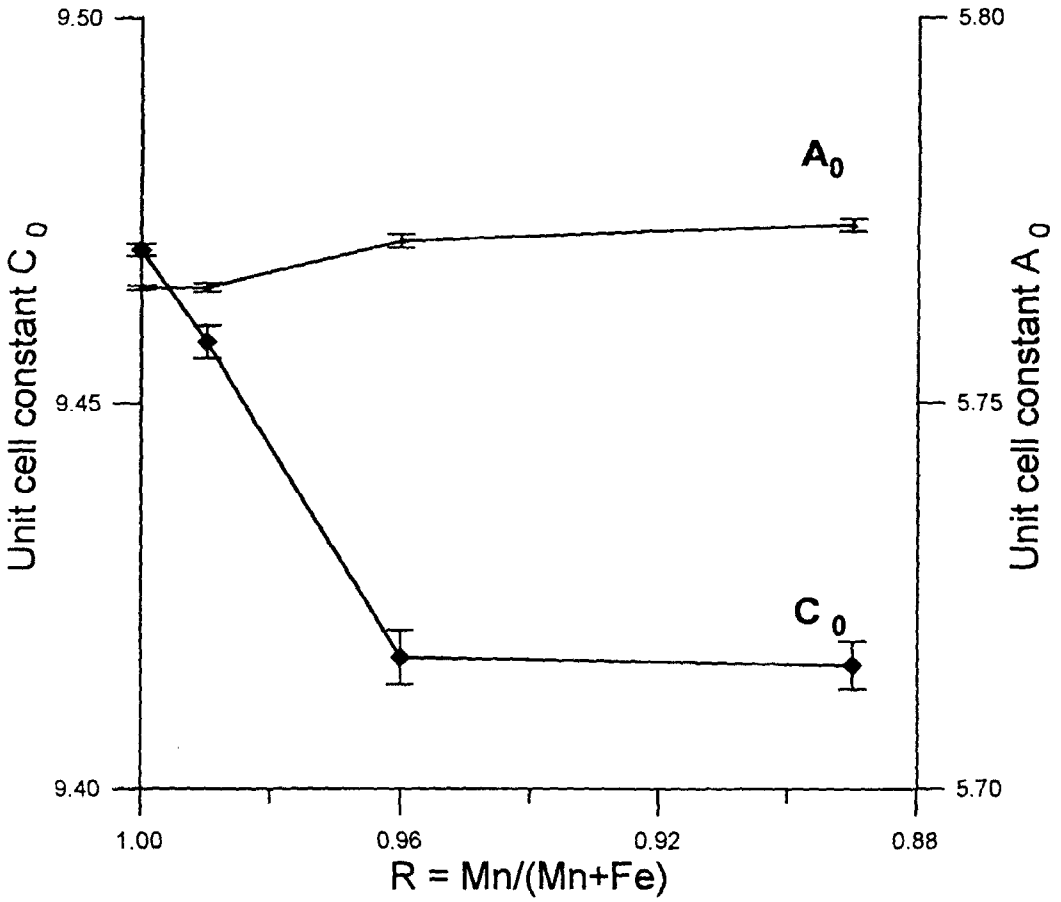


FIG. 5. Variation of unit cell parameters $a_0$ and $c_0$ of hausmannite with decreasing parameter $R$ = Mn/(Fe+Mn) e.g. increasing iron content.

(magnetic and non-magnetic separates of two ore samples and as reference a non-magnetic hausmannite crystal from a vug in Wessels mine) are listed and compared to synthetic $Mn_3O_4$ in Table 1. The charge balance between $Mn_2O_3$ and MnO was calculated following Kleyenstüber (1984). The results indicate that the magnetic hausmannite is iron-rich with $Fe_2O_3$ contents in order of 3–12 wt.%. In contrast non-magnetic fractions contain between 1 and 5 wt.% $Fe_2O_3$ (Fig. 4*a*). Mössbauer spectroscopy on a grain separate of magnetic hausmannite indicated that all iron is present in the trivalent state. Magnesium concentrations are very low (less than 1 wt.% MgO). The distribution of magnesium between magnetic and non-magnetic concentrates appears erratic (Fig. 4*b*).

## Crystallography

X-ray powder diffraction analyses were undertaken on mineral separates with different iron contents in order to obtain information on possible changes of unit cell dimensions as a result of exchange of Mn by Fe. A Philips PW 1710 based vertical goniometer equipped with an iron tube was used. The scan speed was 0.004° $sec^{-1}$ and data were collected from 20 to 140° 2θ. During this exercise the diffractometer was calibrated with an external standard (NBS 640b, silicon) to an accuracy of 0.01° 2θ deviation in the range of data acquisition. The same material was added as an internal standard to the pressed mounts to perform a zero point refinement prior to unit cell constant calculation. Cell constants of the different

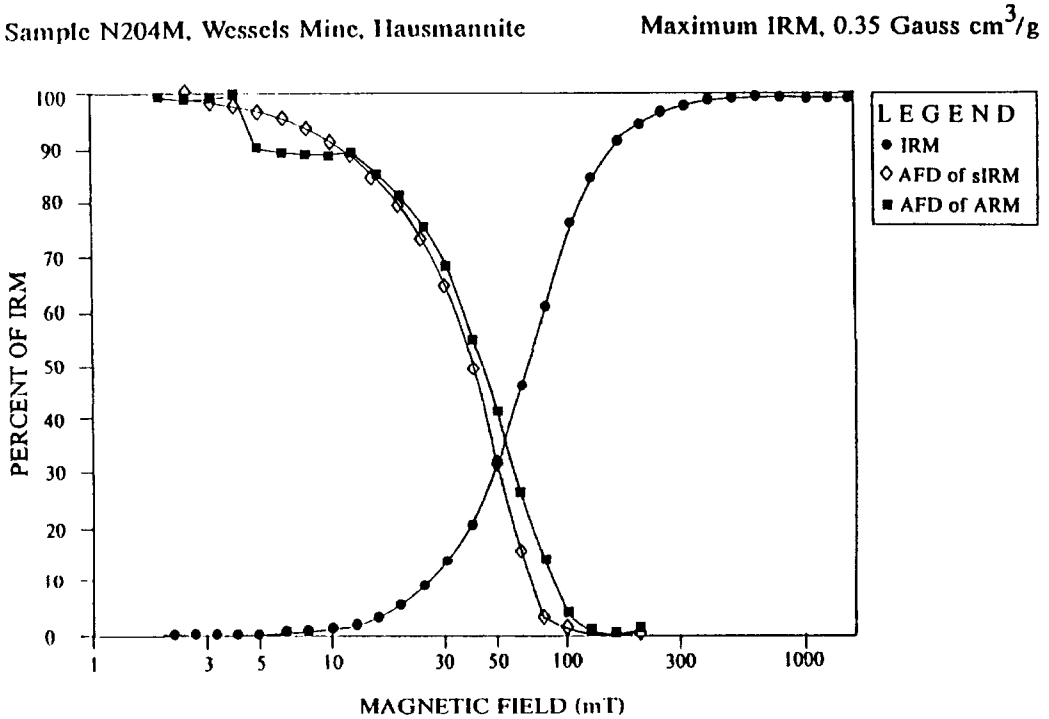


FIG. 6. Coercitivity spectrum of hausmannite sample N205 (block sample). Triangles are for IRM acquisition, solid squares for AF demagnetization, and open squares for AF demagnetization of ARM.

hausmannite samples were calculated from 20 peak positions of the powder pattern with the PC-version of the Appleman-Evans program (Benoit, 1987). Patterns are recorded in Table 2; Table 1 includes the calculated unit cell constants for the different samples.

A small increase of the cell parameter $a_o$ and a much larger decrease of $c_o$ (resulting in a distortion parameter $c_o/a_o$ closer to 1) are observed in the magnetic hausmannite samples (N204, N205) relative to the non-magnetic samples (synthetic $Mn_3O_4$ and LVB4-04) (Fig. 5). However, there is only a marginal difference between the unit cell parameters of the two magnetic samples, indicating that the change of the cell parameters does take place in discrete steps and not gradually with increasing iron content.

## Magnetic mineralogy

Magnetic mineralogy of grain separates and block samples was determined by one of the authors (N.J.B.) in the laboratories of J. Kirshvink at the California Institute of Technology. Coercivity spectra were acquired (Fig. 6) and samples were demagnetized thermally through step heating under atmospheric conditions (Fig. 6).

Studies of magnetic and non-magnetic concentrates showed that separation between different generations of hausmannite was not completely accomplished. So called 'non-magnetic' concentrates have similar characteristics as the 'magnetic' concentrates although on a much lower absolute magnetic level (Fig. 7).

The coercitivity spectrum of the magnetic hausmannite is very similar to that of magnetite as reported by Yamazaki *et al.* (1991) (Fig. 6). Natural remanent magnetization (NRM) of small block samples are in the order of 0.002–0.1 Gauss $cm^3\ g^{-1}$. Isothermal remanent magnetization curves (IRM) are characterized by a steep initial increase and saturation at applied magnetic field strength of 0.25 to 0.5 T. Moments of IRM acquisition reached maxima of between 0.15 and 0.67 Gauss $cm^3\ g^{-1}$. Positive isothermal Laurie-Fuller tests suggest that the remanent magnetization is dominantly carried by single domain hausmannite crystals. Perturbations at low field strength are probably grain size related.

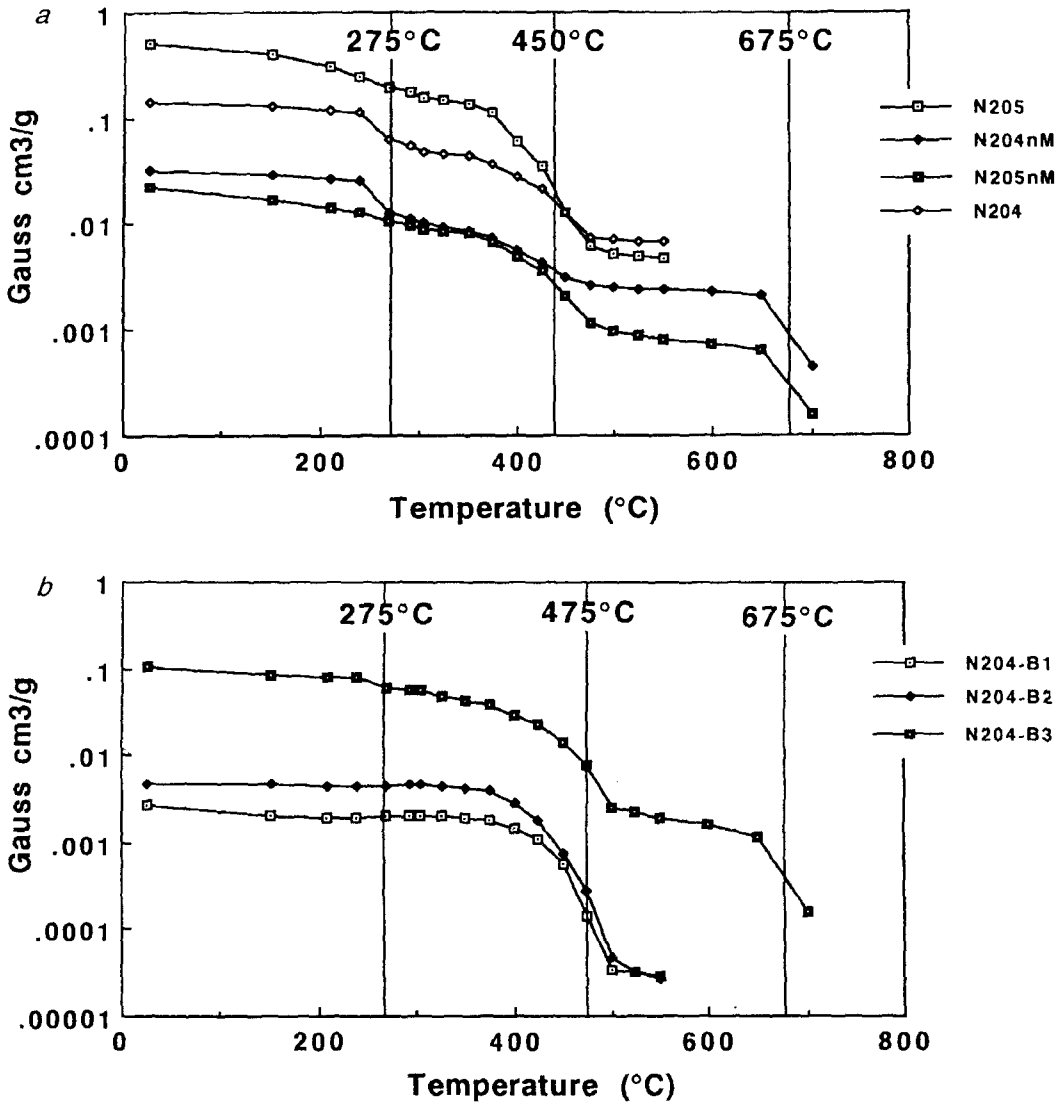


FIG. 7. Thermal demagnetization data of powdered magnetic (M), and non-magnetic (nM) separates (*a*), and blocks (*b*) of samples N204 and N205. Marked are losses of magnetization at 275, 450–475 and 675°C. These correspond to soft demagnetization of multidomain hausmannite grains, the demagnetization of magnetic hausmannite, and the demagnetization of small amounts of hematite respectively.

Blocking temperatures, which appear in the thermal demagnetization curve (Fig. 7) as points of major loss of magnetization, approximate the Curie temperature of the demagnetized phase (Butler, 1992). They consistently fall in in the range of 720–775 K (450–500°C). Small kinks in the demagnetization curve occur also at about 530–550 K (260–280°C) and 920–970 K (650–700°C). The kink at 920–970 K is the result of demagnetization of hematite inclusions in hausmannite grains. Magnetism due to hematite normally accounts for less than one percent of the initial NRM (natural remanent magnetism) of block samples or magnetic separates. The cause for the drop of magnetization

TABLE 3. Intrinsic properties of hausmannite-magnetite series ferrites. Data from Goodenough (1966), Olés et al.(1976); data for iwakiite from Matsubara et al. (1979), for hausmannite from NBS (1972) (lattice constants) and Boucher et al. (1970) (spin configuration), for magnetic hausmannite sample N205, this study

| | Hausmannite | Magnetic hausmannite | Synthetic ferrite | Synthetic ferrite | Iwakiite | Jacobsite | Magnetite |
|---|---|---|---|---|---|---|---|
| Composition | $Mn^{2+}Mn_2^{3+}O_4$ | $Mn^{2+}(Mn,Fe)_2^{3+}O_4$ | $Mn^{2+}Mn^{3+}FeO_4$ | $Mn_2FeO_4$ | $MnFe_2O_4$ | $MnFe_2O_4$ | $Fe^{3+}(Fe^{2+},Fe^{3+})_2O_4$ |
| Site occupation | normal | normal (?) | normal or partly inverted | normal or partly inverted | ? | normal or partly inverted | inverted |
| Crystallographic system | tetragonal | tetragona | tetragonal | cubic | tetragonal | cubic | cubic |
| Unit cell constants (Å) | $a$ = 5.7621<br>$c$ = 9.4696<br>$c/a$ = 1.638 | $a$ = 5.772<br>$c$ = 9.416<br>$c/a$ = 1.631 | $a$ = 8.34<br>$c$ = 8.88<br>$c/a$ =1 .06 | $a$ = 8.49 | $a$ = 8.52<br>$c$ = 8.54<br>$c/a$ = 1.002 | $a$ = 8.52 | $a$ = 8.40 |
| Magnetism | | | | electron spin only | | | |
| Type of magnetic order | similar to Yafet-Kittel order | Yafet-Kittel or Neel order (?) | Neel order | Neel order | ? | Neel order | Neel order |
| A-B spin orientations | 8 discrete directions of spin orientation | ? | antiparallel in (001) | antiparallel | ? | antiparallel | antiparallel |
| Curie temperature (K) | 42.5 | 750 | 413 | ? | ? | 563 | 858 |

530–550 K remains uncertain, but may be related to soft magnetism in multidomain hausmannite grains.

## Discussion

Good introductions into the magnetic properties of Fe–Mn spinels, so-called ferrites, are provided by Smit and Wijn (1959) and Goodenough (1966) and a detailed description of the properties of the physical and chemical properties of hausmannite is given by Frenzel (1980). Data of well studied members of the Mn–Fe spinels are listed in Table 3. Hausmannite has a tetragonally distorted structure and may be compared to more iron-rich members of the group of ferrites (Table 3). Half of the octahedrally coordinated interstices in the f.c.c. oxygen lattice are occupied by trivalent manganese and one eighth of the tetrahedrally coordinated sites are occupied by divalent manganese cations. The tetragonal lattice distortion is an expression of a cooperative Jahn-Teller effect around the octahedrally coordinated $Mn^{3+}$ sites, stretching the spinel-lattice along (001). The degree of inversion is commonly small (Wickham, 1969). The oxygen parameter *u*, a measure for non-stoichiometry, may be a function in understanding the physical properties of hausmannite (Wickham, 1969; Tanaka, 1974), but it is not well studied.

The lattice distortion diminishes with increasing amounts of iron in the compositional series between $Mn_3O_4$ and $Fe_3O_4$ and it disappears at compositions $Mn_2FeO_4$ and $MnFe_2O_4$, where cubic, as well as slightly distorted modifications are known (Table 3) (Goodenough, 1966; Matsubara *et al.*, 1979).

Ferrimagnetism in Mn-Fe spinels is caused exclusively by the orientation of bonding electron spin moments of the cations. The so called orbital magnetic moment is effectively quenched in these compounds (Goodenough, 1966). Only the spins of unpaired electrons can contribute to the magnetic moment of a molecule. Manganese and iron are both transitional metals with 7 and 8 outer electrons respectively in 3*d* and 4*s* orbitals. Their divalent and trivalent cations therefore have electron configurations with 4 ($3d^4$, $3d^6$) or 5 ($3d^5$) unpaired electrons resulting in large theoretical magnetic moments and high Curie constants (Table 4). $Mn^{2+}$ and $Fe^{3+}$ have identical electron configurations and therefore identical magnetic properties. The latter is also true for $Mn^{3+}$ and $Fe^{2+}$ which have equivalent electron configurations with respectively four and six electrons in the outer *d*-orbital.

The magnetic structure of hausmannite below the Curie point is fairly complex (Kasper, 1959; Boucher *et al.*, 1970; Bonnet *et al.*, 1974). According to Boucher *et al.* (1970) the electron spins of the B-site cations form an umbrella of two-fold symmetry around [010] with six distinctive spin orientations. In contrast the electron spins of the *A*-site cations are orientated into two distinctive directions antiparallel to [010]. The magnetic structure of hausmannite has therefore to be described in an orthorhombic cell doubled along [010] relative to the crystallographic cell. The two crystallographic sublattices A (tetrahedrally coordinated) and B (octahedrally coordinated) have to be subdivided into 2 distinctive *A*-site sublattices (*T*1–*T*2) and 6 distinctive *B* sublattices (O1–O6), each characterized by a distinctive direction of spin orientation (Boucher *et al.*, 1970). However, projected onto (001) (Fig. 8*a*) this structure resembles that of a plane triangular Yafet-Kittel spin configuration (Fig. 8*b*). This is in contrast to the simple antiparallel Neel configuration (Fig. 8*c*) of the two crystallographic sublattices characteristic for all other ferrites (Table 3).

The bonding electrons of the cations of different sublattices interact via next-neighbour cation–anion–cation superexchange (Goodenough, 1966; Smit and Wijn, 1959). This coupling is stronger the smaller the distance between cations and oxygen and the closer the angle between the two cation-oxygen bond is to 180° (Smit and Wijn, 1959).

The ordering of the electron spins, by magnetic coupling, is disturbed by thermal excitation. Transformation from the state of ordered spins to the paramagnetic state of disordered spins occurs at the so called Curie point, a material specific temperature. The Curie temperature is therefore a measure of the strength of magnetic coupling. This coupling appears to be very weak in the case of the

TABLE 4. Intrinsic properties of the divalent and trivalent cations of iron and manganese

| Cation | $Mn^{2+}$ | $Mn^{3+}$ | $Fe^{2+}$ | $Fe^{3+}$ |
|---|---|---|---|---|
| Ionic radius (pm) | 83 | 66 | 78 | 65 |
| Orbital electron configuration | $3d^5$ | $3d^4$ | $3d^6$ | $3d^5$ |
| Bonding electron configuration | $t_{2g}^4\ e_g^2$ | $t_{2g}^3 e_g^1$ | $t_{2g}^6\ e_g^0$ | $t_{2g}^4\ e_g^2$ |
| Theoretical magnetic moment ($\mu_B$) | 5 | 4 | 4 | 5 |
| Curie constant per gram ion | 4.38 | 3.00 | 3.00 | 4.38 |

complex magnetic structure of iron-free hausmannite, resulting in a very low Curie temperature of 40–45 K. However, the coupling apparently becomes stronger in compounds where manganese is replaced by iron, as suggested by increasing Curie temperatures of ferrite compounds with simple Neel ordering with diminishing manganese content. It is for example 858 K in magnetite (Table 3).

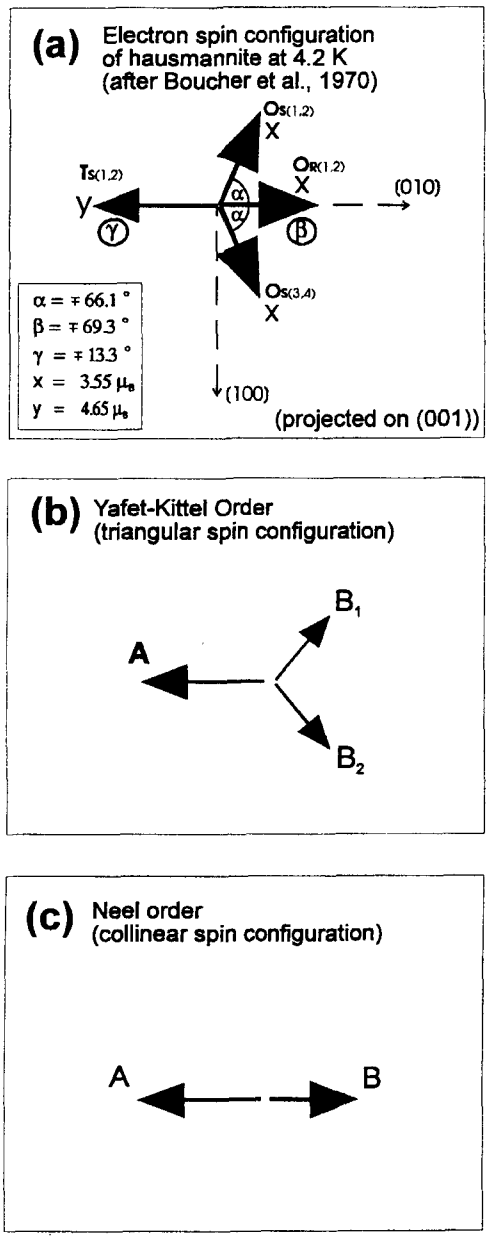


The same principle may apply to the iron-rich magnetic hausmannite with unknown magnetic order scheme. With an iron content of a few weight percent stability of the ferrimagnetic state. e.g. strong coupling of electron spins, may be accomplished and the Curie temperature increased from 40–45 K to 750 K, i.e. not far off from the Curie temperature of magnetite. The $Mn^{3+}$–$Fe^{3+}$ exchange apparently enforces the spin coupling and stabilizes the ferrimagnetic state (Fig. 8*a*). This stabilization could result from simplification of the magnetic ordering from Yafet-Kittel to Neel order or simply from stronger spin coupling between individual cation sites due to increase of the mean magnetic moment.

The magnetic hausmannite is distinctively different from ordinary hausmannite not only in its magnetic properties but also in its remarkably high iron content and its unit cell parameters. The iron content can be expressed in the parameter $R$ = Mn/(Mn+Fe). $R$ reaches a minimum value of 0.89 in the magnetic hausmannite (12 wt.% $Fe_2O_3$). This is considerably lower than $R$ = 0.93 (or 6.9 wt.% $Fe_2O_3$) envisaged by Mason (1943), Van Hook and Keith (1958), Halba *et al.* (1973), and Osawa *et al.* (1992) as the room temperature stability limit for the solubility of iron in the hausmannite lattice in the system $Mn_3O_4$–$MnFe_2O_4$. The composition reported for the magnetic hausmannite falls, according to all these studies, into the two-phase region, the single phase 'magnetic hausmannite' should therefore be unstable. However, the observed change of the unit cell parameters for magnetic hausmannite relative to non-magnetic hausmannite, may indicate a distinct change within the crystal structure due to the high iron content.

Unfortunately no other quantitative conclusion can be drawn, as neutron diffraction data to determine the exact spin configuration and the distribution of iron and manganese between the different lattice sites are not available at this stage. Work is in progress to obtain such information; however, it remains a major problem to obtain pure phases suitable for analysis.

FIG. 8. (*a*) The electron spin configuration of hausmannite at 4.2 K after Boucher *et al.* (1970), projected on (001). Eight discrete directions of electron spin orientation (equivalent to eight magnetic sublattices) are notable, six of these ($O_1$–$O_6$) of cations in octahedral coordination, two ($T_1$, $T_2$) of cations in tetrahedral coordination. (*b*) Yafet-Kittel model of triangular spin ordering in a two-sublattice mode, resembling the projection of the hausmannite configuration. (*c*) Simple antiparallel Neel order with collinear electron spins in a two-sublattice mode. This model is valid for $Mn_3O_4$-$Fe_3O_4$ series ferrites with the exeption of hausmannite.

## Conclusions

Unusually magnetic hausmannite, which clings to a hand magnet, is present in hydrothermally altered sedimentary manganese ores of the Kalahari manganese deposit in South Africa. The magnetic hausmannite is very fine-grained and intergrown with coarse-grained, non-magnetic hausmannite in the manganese ores. The only impurities present in the magnetic hausmannite are small inclusions of hematite. The magnetic hausmannite is enriched in iron relative to non-magnetic hausmannite and occurs immediately adjacent to ferruginized fault zones in the manganese field.

The magnetic hausmannites have thermal blocking temperatures, approximating the Curie temperature, of about 750 K. This is in contrast to pure iron-free hausmannite with Curie temperatures of 40–45 K. The high blocking temperature appears to be related to the increased iron contents in the hausmannite. Exchange of manganese by iron in hausmannite may stabilize ferrimagnetic ordering in the crystal structure and increase the temperature at which transformation from the ferrimagnetic state to the paramagnetic state (the Curie temperature) takes place. A similar effect is seen in other spinels with Neel ordering, where Curie temperature increases from 563 K in jacobsite to 858 K in magnetite.

Knowledge of the characteristics and the distribution of the magnetic hausmannite may in future be of value in geophysical exploration for high-grade ores in the Kalahari manganese field. Also, recognition of the magnetic hausmannite phase indicates that there may be need for careful examination of the magnetic properties of hausmannite from other manganese deposits. In this connection it is interesting to note that Fan *et al.* (1993) describe a jacobsite-type phase with compositional and magnetic properties fairly similar to the magnetic hausmannite described here.

## Acknowledgements

Special thanks to Joe Kirshvink (CALTECH) for supporting studies by one of us (N.J.B.) at his laboratory. Thanks also to Ina Penberthy (MINTEK) for performing the image processing on the SEM and to Faan Waanders (Potchefstroom University) for doing Mössbauer spectroscopy on the hausmannite. We are indebted to Hendrik Alberts (RAU) for constructive discussions about the magnetic properties of spinels.

## References

Benoit, P.H. (1987) Adaption to microcomputer of the Appleman-Evans program for indexing and least-square refinement of powder-diffraction data for unit-cell dimension. *Amer. Mineral.*, **72**, 1018–9.

Beukes, N.J. (1983) Palaeoenvironmental setting of iron formations in the depositional basin of the Transvaal Supergroup, South Africa. In *Iron formations, facts and problems* (A.F. Trendall and R.C. Morris, eds.). Elsevier, Amsterdam: 131–209.

Bonnet, A., Delapalme, A. and Tcheou, F. (1974) In *Proceedings of the International Conference on Magnetism*, **5**, 605.

Boucher, B., Buhl, R. and Perrin, M. (1970) Proprietes et structure magnetique de $Mn_3O_4$. *J. Phys. Chem. Sol.*, 32,.2429–37.

Butler, R.F. (1992) *Palaeomagnetism*. Blackwell, Cambridge, 319 pp.

Fan, D., Hariya, Y., Li, J., Miura, H., and Ye, J. (1993) Study on strongly metamorphosed ferro-manganese oxide minerals in Wafangzi deposit, P.R. China. *Resource Geol.*, **17**, 50–6.

Frenzel, G. (1980) The manganese ore minerals. In *The geology and geochemistry of manganese* (I.M. Varentsov and G. Grasselly, eds.). Schweizerbarth, Stuttgart, **1**, 25–157.

Goodenough, J.B.(1966) *Magnetism and the chemical bond*. Interscience Publishers, New York, 393 pp.

Gutzmer, J. (1993) *Hydrothermale Alteration von Manganerzen der Nchwaning Mine, Kalahari Manganerzfeld*, Südafrika. M.Sc. thesis (unpubl.), TU Clausthal, Clausthal-Zellerfeld, 161 pp.

Gutzmer, J. and Beukes, N.J. (1993) Fault controlled hematitization and upgrading of manganese ores in the Kalahari manganese field, South Africa. In *Extended Abstracts 16th Colloquium of African Geology*, (R. Maphalala and M. Mabuza, eds.). Geological Survey and Mines Mbabane, Swaziland, 139–41.

Halba, P., Khilla, M.A. and Kripicka, S. (1973) On the miscibility gap of spinels $MnxFe_{3-x}O_{4+y}$. *J. Phys. Chem. Sol.*, **34**, 387–95.

Kasper, J.S. (1959) Magnetic structure of hausmannite, $Mn_3O_4$. *Bull. Amer. Phys. Soc.*, Series 2, **4**, 178.

Kleyenstüber, A.S.E. (1984) *A regional mineralogical study of the manganese bearing Voelwater Subgroup in the Northern Cape Province*. PhD thesis (unpubl.), RAU, Johannesburg, 328 pp.

Mason, B. (1943) Mineralogical aspects of the system $FeO–Fe_2O_3–MnO–Mn_2O_3$. *Geol. Foren. Forhandl.*, Norway, **65**, 95 – 180.

Matsubara, S., Kato, A. and Nagashima, K. (1979) Iwakiite, $Mn^{2+}(Fe^{3+}, Mn^{3+})_2O_4$, a new tetragonal spinelloid mineral from the Gozaisho mine, Fukushima Prefecture. *Mineral. J. Japan*, **9**, 383.

National Bureau of Standards (U.S.) (1972) *National Bureau of Standards Monograph*, **25**, 38.

Nel, C.J., Beukes, N.J. and De Villiers, J.P.R. (1986) The Mamatwan mine of the Kalahari manganese field. In *Mineral deposits of Southern Africa* (C.R. Anhaeusser and S. Maske, eds.). **1**, 963–78.

Osawa, S., Kikuchi, T. and Hariya, Y. (1992) Phase equilibria in the system $MnFe_2O_4$ – $Mn_3O_4$. *Mineral. J. Japan*, **16**, 28–39.

Olés, A., Kajzar, F., Kucab, M. and Sikora, W. (1976) *Magnetic structures determined by neutron diffraction.* Warzow, 727 pp.

Smit, J. and Wijn, H.P.J. (1959). *Ferrites*. Philips Technical Library, Almeloh, 369 pp.

Tanaka, T. (1974) Lattice constant and nonstoichiometry in Mn-Fe ferrites. *Japan. J. Appl. Phys.*, **13**, 1235–7.

Van Hook, H.J. and Keith, M.L. (1958) The system $Mn_3O_4$–$Fe_3O_4$. *Amer. Mineral.*, **43**, 69–83.

Wickham, D.G. (1969) The chemical composition of spinels in the system $Fe_3O_4$–$Mn_3O_4$. *J. Inorg. Nucl. Chem.*, **31**, 313–20.

Yamazaki, T., Katsura, I. and Marumo, K. (1991) Origin of stable remanent magnetization of siliceous sediments in the central equatorial Pacific. *Earth Planet. Sci. Lett.*, **105**, 81–93.

[*Manuscript received 6 February 1995: revised 27 March 1995*]